

PBDOWN — A Computer Code for Simulating Core Material Discharge and Thermal to Mechanical Energy Conversion in LMFBR Hypothetical Accidents

P. Royl

*Institut für Reaktorentwicklung, Kernforschungszentrum
Karlsruhe GmbH, Postfach 3640, D-7500 Karlsruhe, Germany*

PBDOWN is a computer code that simulates the blowdown of confined boiling materials ("pools") into a colder upper coolant plenum as time dependent ejection and expansion with consideration of a few selected exchange processes. Its application is restricted to situations resulting from hypothetical loss of flow (LOF) accidents in LMFBR's, where enough voiding has occurred, that in core sodium vapor pressures become negligible. PBDOWN considers one working fluid for the discharge process (either fuel or steel) and a maximum of two working fluids (either fuel and sodium or steel and sodium) for the expansion process in the upper coolant plenum. Entrainment of sodium at the accelerated bubble liquid interfaces is mechanistically calculated by a Taylor instability entrainment model. Simulation of a hemispherical expansion form together with this mechanistic entrainment model gives a new integrated calculation of the time dependent sodium mass in the bubble. The paper summarizes the basic equations and assumptions of this computer model. Sample results compare different heat transfer and Na entrainment models during steel and fuel driven discharge processes. Mechanistic sodium entrainment simulation for SNR-type reactors coupled with a realistic heat transfer model is shown to reduce the integral mechanical work potential by a factor of 1.3 to 2.0 over the isentropic energy of the discharge working fluids.

1. Introduction

Analysis of hypothetical core disruptive accidents (HCDA's) in LMFBR's involves simulation of sequences in which confined boiling core materials ("pools") are discharged into the upper coolant plenum. Here they expand further, interact with sodium, and solidify before they settle as particulate debris. Both the material discharge and the expansion in the upper plenum involve complicated multiphase multicomponent exchange processes. Their integrated simulation is very complicated [1]. Analyses giving conservative estimates for the resulting mechanical energy source term are therefore made for the more effective working fluids fuel, steel, and sodium for instance by calculating isentropic expansion energies. PBDOWN (Pool Blow Down) is a computer model which simulates this material discharge as a time dependent ejection and expansion with special consideration of a few selected exchange processes. It allows one working fluid for the discharge process (either fuel or steel) and a maximum of two working fluids for the expansion process in the upper coolant plenum (either fuel and sodium or steel and sodium). The model concentrates in particular on simulation of thermal interactions of the entrained sodium in the expanding bubble with the discharged core materials, on the pressure vs. time behaviour and the resulting mechanical energy potential. The expansion geometry is simple. Upper core and upper internal structures above the ejection orifice which can play an important role in dissipating energy of the ejected materials are neglected.

2. Overview over Modeling and Assumptions

PBDOWN simulates a boiling pool and an expanding multiphase bubble as two homogeneous zones which are connected through an orifice (fig. 1). The model goes beyond similar earlier work of Cho [2] and Corradini [3]. Its mass and energy equations are generalized to the system fuel and steel in the pool and fuel, steel, and sodium in the bubble. Whenever the pool pressure exceeds the bubble pressure pool material is ejected applying quasistationary flow correlations. Expansion of the bubble occurs with a stepped up constraint model for the acceleration of the coolant in the upper plenum which is adjusted to the SNR-300 geometry. This model includes a hemispherical expansion phase in which a generalized Rayleigh momentum equation is solved with a volume source term. The entrained coolant volume which can reach considerable liquid volume fractions in the bubble does not add to the pressure volume work. The model enforces a compatibility between the ejected and entrained masses and the available volumes in the

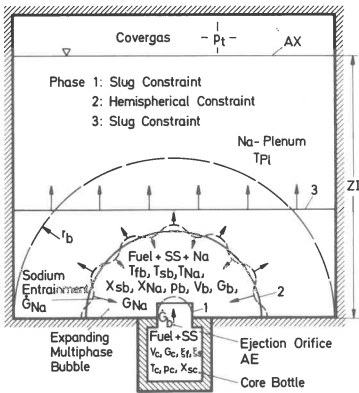


Fig. 1: Basic Features of PBDOWN

bubble. Subcooled sodium enters the bubble at the accelerated vapor liquid interfaces with a rate that can be determined from different entrainment models. Besides using a parametric model PBDOWN allows also for a mechanistic entrainment calculation from the coolant acceleration based on Corradini's Taylor instability entrainment model [3]. Its application in the hemispherical expansion phase can add substantial amounts of sodium before entrainment cut off occurs due to negative accelerations at the bubble liquid interface resulting at high expansion velocities. The treatment of the hemispherical expansion form which has been observed in related experiments [4] coupled with a Taylor instability entrainment mechanism provides a new

integrated simulation of the time dependent sodium mass in the bubble where the thermal interaction with the ejected materials can be enhanced due to entrainment interruption [5]. Heat exchange and vaporization of the entrained sodium is simulated to be condensation controlled with an instantaneous heat up of the entrained sodium to saturation conditions and a subsequent rate dependent radiative and/or conduction controlled vaporization [2], or else to be a radiation and vapor diffusion controlled rate dependent energy transfer both above and below the saturation temperature [3]. The evaporated sodium is instantaneously superheated to thermal equilibrium with the vapor of the ejected component. The nonequilibrium between sodium vapor and liquid is derived from the physical picture of a boundary layer of pure saturated sodium vapor around the sodium droplets, so that the Na saturation temperature follows the total bubble pressure [2]. The governing equations for PBDOWN are summarized in appendix A which also explains the nomenclature. Besides the general conditions for the model defined above the equations are based on the following simplifying assumptions:

1. The specific volume of the liquid phase is negligible compared to that of vapor
2. Heat transfer between fuel and steel is simulated in the bubble while thermal equilibrium is assumed within the pool. Fuel is treated as a single phase liquid in a fuel steel mixture.
3. The vapor components behave as an ideal gas
4. Specific heat, latent heat of vaporization and liquid densities are constant
5. Vapor pressure changes are described by the Clausius Clapeyron equation

The postulated equilibrium condition in the pool exaggerates heat exchange of fuel and steel in a steel driven discharge. The ejected fuel in a fuel steel mixture transfers energy to the steel with an exchange coefficient taken from ref. [1]. It does not interact directly with the liquid sodium. The equations from appendix A form a complete set that defines and couples the pool, bubble, slug, constraint, and covergas conditions. Numerical integration is performed for the increments in temperatures, vapor qualities, and bubble volume using mean values for the integral quantities over each time step and a time step modification scheme. Compatibility of the temperatures and vapor qualities in the bubble with the integral condition from eq. (12), after Na saturation also with the nonequilibrium conditions from eqs (8) and (25) is enforced for each time step. The increments are corrected with conservation of the transferred energy in the sodium and fuel or steel component. Special solutions are applied when fuel or steel approach the sodium temperature or for the case where sodium is condensed due to large entrainment rates.

3. Results

A comparison of different heat transfer and Na entrainment models has been made with PBDOWN for a steel driven discharge of a fuel-steel mixture after the transition phase of a LOF accident and for a fuel vapor driven discharge of fuel after an energetic disassembly phase induced by sodium voiding in a LOF accident (Fig. 2). A range of initial average pool temperatures was investigated which goes far beyond what is mechanistically achievable in such hypothetical accidents. It demonstrates the relative differences between these models at various temperature levels. Compression of the covergas was neglected since analysis showed little influence on the overall energy conversion. Discharge was simulated with the blowdown correlation from Fauske eq. (21). The total core cross section was used as an ejection orifice which pessimisti-

cally maximizes the rate of enthalpy transport into the bubble. The masses and geometries are representative for SNR-300 type reactors. The fuel mass is slightly less than in the CRBR, for which similar fuel vapor driven blowdown calculations have been performed by Corradini [3].

Compared to these calculations for the CRBR two important differences exist however in the geometry for the expansion process, i.e. the cross sectional area of the sodium slug above the core is only half as big in the SNR due to the presence of the shield tank and the considered final expansion volume of 70 m^3 is more than 3 times larger. The bigger expansion volume increases the expansion time and the potential of sodium as a working fluid. The smaller slug cross section reduces the entrainment surface and decreases the attainable sodium to fuel mass ratios for the same expansion time which enhances the work potential, if one compares with the CRBR results. The Taylor instability entrainment model with the stepped up constraint phases from PBDOWN was applied with four different heat transfer simulations and compared to results without entrainment and to the isentropic expansion energies. In case of the fuel-steel mixture these were pessimistically calculated assuming thermal equilibrium between the two components. Besides that results are also given for the Cho model [2] with the most energy enhancing entrainment rate of 0.2 and with blackbody radiation and heat conduction for very small Na-droplets of 0.007 cm radius. This last model (cases S1 and F1) yields the highest work potentials, although only a small fraction of the core inventory gets involved. Energies can increase by a factor of 1.6-1.7 above the isentropic values for the SNR geometry. This parametric simulation and the large heat transfer rates are unrealistic, however.

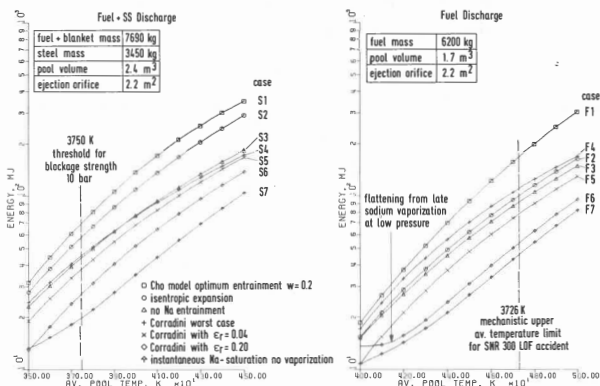


Fig. 2: PBDOWN Work Potentials at 70 m^3 Expansion Volume

Heat transfer for sodium vaporization was controlled by radiation onto a clean sodium surface for which a radiative absorptivity of $\epsilon_r = 0.04$ was applied. For fuel vapor this so called worst case simulation resulted in energies slightly below the isentropic values in Corradini's expansion analysis for the CRBR [3]. For the SNR geometry it leads to energies ca. 10% above the isentropic values. Part of this increase comes from the reduced Na entrainment in the hemispherical constraint phase, which was not accounted for in the earlier analysis. For the steel driven discharge this approach as all the others except the Cho model results in a reduction of the work potential over the isentropic value because the thermal contact between the fuel and steel is essentially lost after discharge into the upper plenum. The assumption that the entrained sodium is raised instantaneously to saturation uses the physical picture of a rapid heat transfer due to condensation of fuel or steel vapor on the droplet surfaces. As

shown in ref. [3] this vapor condensation is inhibited by early sodium vapor generation. A gas layer is rapidly built up which acts as a noncondensable gas. It reduces heat transfer to the sodium to a diffusion controlled condensation with a smaller heat transfer rate than due to radiation from the condensed fuel or steel fog around this vapor layer. Both mechanisms are combined in a more realistic model from Corradini eq. (19). Using this model in the expansion simulation makes the sodium dominantly act as a heat sink, where smaller absorptivities of the sodium surface degrade the work potential less. This reasonable heat transfer model with $\epsilon_r = 0.04$ (cases S5 and F5) leads only to a small reduction over the expansion energy without sodium entrainment (cases S3 and F3). Using an absorptivity of 0.2, which corresponds to a partly dirty droplet surface, transfers more energy to the sodium (cases S6 and F6). Vaporization of sodium does occur in this case shortly before reaching the expansion volume of 70 m^3 . Its contribution to the work potential is small. Only for mild discharge processes at low initial fuel temperatures and vapor pressures it causes the flattening in case F6. All energies in fig. 2 do not drop under the lower limit for the possible degrading effect of sodium entrainment on the overall expansion energy (cases S7 and F7). As in ref. [3] this limit was obtained under the assumption of an instantaneous sodium heat up to saturation without any vaporization.

4. Conclusions

Time dependent discharge through the maximum available core opening and a mechanistic sodium entrainment simulation coupled with a reasonable heat transfer model can altogether reduce the energy of blowdown events in the discharge phase of hypothetical LOF accidents in SNR-type reactors by a factor of 1.3 to 2.0 compared to the isentropic values. Pessimistic worst case calculations, if they are based on a mechanistic entrainment simulation, have only a small potential for enhancing the expansion energy even if the entrainment rate is intermediately cut down during the phase of hemispherical expansion. The pessimistic amplification factor of 1.1 results in this case to some degree from the large expansion volume in the SNR-300 which allows for a greater contribution of the sodium vapor expansion at lower pressures to the overall work potential. The stepped up constraint model and the entrainment surface in PBDOWN have been selected with plausible criteria derived from the SNR-300 vessel geometry. But the calculated entrained volume fractions are still lower than what is known from available experiments [4]. For an improved analysis that takes credit from the expected larger entrainment rates one must wait till results from scaled experiments for this geometry become available to which the open model parameters such as constraint sequences and entrainment mechanisms can be adjusted.

5. References

- [1] Bell, C.R. et al.: "Impact of SIMMER-II Model Uncertainties on Predicted Post Disassembly Dynamics", LA-8053-MS, NUREG/CR-1058 Oct. 1979
- [2] Cho, D.H. and Epstein, M.: "Work Potential Resulting from a Mechanical Disassembly of the voided FFTF Core". ANL/RAS 74-17, Argonne 1974
- [3] Corradini, M.L.: "Heat Transfer and Fluid Flow Aspects of Fuel Coolant Interactions", PHD thesis COO-2781-15 TR, Massachusetts Institute of Technology (1978)
- [4] Moszynski, J.R. and Ginsberg, T.: "Liquid Entrainment by an Expanding Gas or Vapor Bubble - A Review of Experiments and Models", BNL-NUREG-28348, Brookhaven 1980
- [5] Buchner, H. and Royl, P.: "Scoping Analysis of Boiling Pool Pressurization and Discharge in the Transition Phase of Hypothetical Loss of Flow Accidents", Procs. Fast Reactor Safety Conference, Seattle 1979, Vol I, p. 150
- [6] Fröhlich, R. et al.: "Status of Hypothetical Core Disruptive Accident Energetics Analysis for Licensing of SNR-300", Trans ANS 35 (1980) p. 379-381
- [7] Fauske, H.K.: "The Discharge of Saturated Water through Tubes", Chemical Engineering Progress, 61 (55), p.210, (1965)

1. Energy of Material in the Pool

$$\frac{d}{dt} [\dot{G}_c (\xi_f e_{fc} + \xi_f e_{fc})] = \frac{d\dot{G}_c}{dt} (\xi_f [e_{fc} + p_c v_{fc}] + \xi_s [e_{sc} + p_c v_{sc}]) + \dot{G}_c (\xi_f q_f + \xi_s q_s) \quad (1)$$

Eq. (1) was rewritten in terms of core temperature and vapor mass fraction and the continuity relation $\dot{G}_c = -\dot{G}_b$ for the mass change by ejection was used to give:

$$(\xi_f c_f + \xi_s c_s - \xi_s x_{s,c} R_s) \dot{T}_c + \xi_s (L_s - R_s T_c) \dot{x}_{s,c} = -\frac{\dot{G}_b}{\dot{G}_c} \xi_s R_s T_c X_{s,c} + (\xi_f q_f + \xi_s q_s) \quad (2)$$

2. Continuity Equation and EOS for Vapor Mass Fraction in the Core

$$\frac{1}{v_c} \frac{dv_c}{dt} = \frac{1}{\dot{G}_c} \frac{d\dot{G}_b}{dt} \quad (3)$$

Rewriting eq.(3) with assumptions 1-5 yields:

$$\frac{1}{T_c} [1 - \frac{L_s}{R_s T_c}] \dot{T}_c + \frac{1}{x_{s,c}} \dot{x}_{s,c} = \frac{\dot{G}_b}{\dot{G}_c} \quad (4)$$

3. Energy of the non Boiling f-Component in the Bubble

$$\xi_f \frac{d}{dt} [\dot{G}_b e_{fb}] = \xi_f \dot{G}_b (e_{fc} + p_c v_c) + \xi_f \dot{G}_b (q_f - h_{eff} (T_{fb} - T_{sb})) \quad (5)$$

Using the relation between enthalpy and internal energy and rearranging leads to the energy equation for the non boiling f-component in the bubble in terms of temperature for this component:

$$C_f \dot{T}_{fb} = \frac{\dot{G}_b}{\dot{G}_b} c_f (T_c - T_{fb}) + q_f - h_{eff} (T_{fb} - T_{sb}) \quad (6)$$

4. Energy of the boiling s-component in the bubble

$$\xi_s \frac{d}{dt} [\dot{G}_b e_{sb}] = \xi_s \dot{G}_b (e_{fb} + p_c v_{sc}) + \xi_s \dot{G}_b (q_s + \frac{q_f}{\xi_s} h_{eff} (T_{fb} - T_{sb})) - \dot{Q}_{s,Na} - p_b \frac{d}{dt} (\xi_s \dot{G}_b v_s) \quad (7)$$

Using assumptions 1, 3, 4, and applying the non equilibrium condition that the liquid sodium saturation temperature always follows the total bubble pressure, once it has reached the saturation is

$$T_{Na} = \frac{H}{K - \ln(p_b)} \quad \text{for } x_{Na} \geq 0.0 \quad (8)$$

and with the definition of eq. (17) for the heat exchange $\dot{Q}_{s,Na}$ between the s-component and the entrained sodium one obtains a modified energy equation in terms of bubble temperatures and vapor mass fractions:

$$C_s \dot{T}_{sb} + L_s \dot{x}_{sb} - x_{sb} R_s T_{sb} \frac{H}{T_{Na}} \dot{T}_{Na} + \frac{\dot{G}_{Na}}{\xi_s \dot{G}_b} (T_{sb} - T_{Na}) \dot{x}_{Na} = \frac{\dot{G}_b}{\dot{G}_b} [C_s (T_c - T_b) - L_s (X_{s,c} - X_{sb})] + q_s + \frac{q_f}{\xi_s} h_{eff} (T_{fb} - T_{sb}) - \frac{1}{\xi_s \dot{G}_b} [\dot{G}_{Na} X_{Na} C_{g,Na} (T_{sb} - T_{Na}) + \dot{Q}_c] \quad (9)$$

5. Energy Equation for the Entrained Sodium in the Bubble

$$\frac{d}{dt} (\dot{G}_{Na} e_{Na}) = \dot{G}_{Na} e_{Na,0} + \dot{Q}_{s,Na} - p_b \frac{d}{dt} (\dot{G}_{Na} v_{Na}) \quad (10)$$

Using the same assumptions as for eq. (9) energy equation of sodium can be rewritten in terms of bubble temperatures and vapor masses:

$$X_{Na} (R_{Na} + C_{g,Na}) \dot{T}_{sb} + [C_{Na} - X_{Na} (R_{Na} + C_{g,Na} + R_{Na} T_{sb} \frac{H}{T_{Na}})] \dot{T}_{Na} + [L_{Na} + R_{Na} (T_{sb} - T_{Na})] \dot{x}_{Na} = \frac{\dot{G}_{Na}}{\dot{G}_{Na}} [X_{Na} (L_{Na} + R_{Na} (T_{sb} - T_{Na})) + C_{Na} (T_{Na} - T_{Na,0})] + \frac{\dot{Q}_c}{\dot{G}_{Na}} \quad (11)$$

6. EOS and Continuity Equation for the s-Vapor Component in the Bubble

$$p_{sb} V_{gas} = x_{sb} \xi_s \dot{G}_b R_s T_{sb} \quad (12)$$

with the gas volume in the bubble determined from the bubble volume by subtracting the liquid content:

$$V_{gas} = V_b - (\xi_f v_f^l + \xi_s (1 - x_{sb}) v_s^l) \dot{G}_b - (1 - x_{Na}) v_{Na}^l \dot{G}_{Na} \quad (13)$$

Using the Clausius Clapeyron equation for the vapor pressure change in the s-component in the time derivative of eq. (12) yields:

$$\frac{1}{T_{sb}} \left(1 - \frac{L_s}{R_s T_{sb}} \right) \dot{T}_{sb} + \left(\frac{1}{X_{sb}} - \frac{\dot{q}_s G_b}{V_{gas}} v_{s1} \right) \dot{X}_{sb} - \frac{G_{Na}}{V_{gas}} v_{Na}^1 \dot{X}_{Na} = \frac{1}{V_{gas}} \dot{V}_b - \left[\frac{1}{G_b} + \frac{\dot{q}_s v_{s1}^1 + \dot{q}_s (1 - X_{sb}) v_{s1}^1}{V_{gas}} \right] \dot{G}_b - \frac{(1 - X_{Na}) \dot{V}_{Na}^1}{V_{gas}} \dot{G}_{Na} \quad (14)$$

7. EOS and Continuity Equation for both Vapor Components in the Bubble

$$P_b V_{gas} = (X_{sb} \dot{q}_s G_b R_s + X_{Na} G_{Na} R_{Na}) T_{sb} = G R_{eff} T_{sb} \quad (15)$$

Rearranging eq. (15) in the same way as eq. (12) and introducing the sodium temperature from eq. (8) for the bubble pressure yields:

$$-\frac{1}{T_{sb}} \dot{T}_{sb} - \left(\frac{R_s}{G R_{eff}} - \frac{v_{s1}^1}{V_{gas}} \right) \dot{q}_s G_b \dot{X}_{sb} + \frac{H}{T_{Na}} \dot{T}_{Na} - \left(\frac{R_{Na}}{G R_{eff}} - \frac{v_{Na}^1}{V_{gas}} \right) G_{Na} \dot{X}_{Na} = -\frac{1}{V_{gas}} \dot{V}_b + \left[\frac{\dot{q}_s X_{sb} R_s}{G R_{eff}} + \frac{\dot{q}_s v_{s1}^1 + \dot{q}_s (1 - X_{sb}) v_{s1}^1}{V_{gas}} \right] \dot{G}_b + \left[\frac{X_{Na} R_{Na}}{G R_{eff}} + \frac{(1 - X_{Na}) v_{Na}^1}{V_{gas}} \right] \dot{G}_{Na} \quad (16)$$

8. Heat Exchange between the s-component and the Entrained Sodium

$$\dot{Q}_{S,Na} = \dot{Q}_l + \dot{Q}_m = \dot{Q}_l + \frac{d}{dt} (X_{Na} G_{Na}) C_{g,Na} (T_{sb} - T_{Na}) \quad (17)$$

Cho-Epstein Model

This model from ref. [2] instantaneously raises the entrained sodium droplet to saturation, vaporizes it rate dependent by radiation and conduction and instantaneously superheats the vapor to thermal equilibrium with the s-component. The first two components are summarized as \dot{Q}_1 with

$$\dot{Q}_l = \dot{G}_{Na} C_{Na} (T_{Na} - T_{Na0}) + \frac{3 G_{Na} (1 - X_{Na}) v_{Na}^1}{R_p} \left[\epsilon_r \epsilon_\tau (T_{sb}^4 - T_{Na}^4) + \frac{R_{g,Na}}{R_p} (T_{sb} - T_{Na}) \right] \quad (18)$$

Corradini Model

This model from ref. [3] simulates heat transfer also to the subcooled entrained sodium as a rate dependent process and simulates vaporization by a diffusion controlled condensation of the s-component on the droplet surface, sodium vapor is again instantaneously superheated to thermal equilibrium with the s-component.

$$\dot{Q}_l = \frac{3 G_{Na} (1 - X_{Na}) v_{Na}^1}{R_p} \left[\epsilon_r \epsilon_\tau (T_{sb}^4 - T_{Na}^4) + \frac{\alpha_{g,Na}}{R_s T_{sb}} \frac{P_{sat,s}(T_{sb})}{R_p} \right] \quad (19)$$

In the Corradini Model T_{Na} can be lower than saturation conditions. In this case the saturation pressure from s becomes the bubble pressure, eqs. (9) and (11) simplify and eq. (16) is not solved at all.

9. Ejection Rate from the Pool into the Bubble

$$\dot{G}_b = \begin{cases} A E \cdot j & \text{when } P_b < P_c \\ 0 & \text{when } P_b \geq P_c \end{cases} \quad (20)$$

Two different models can be applied for the quasistationary blow down of the core materials

$$\text{Fauske ref. [7]:} \quad j = \frac{G_c}{V_c} 0.61 \sqrt{2(P_c - P_x)} \quad \text{with } P_x = \max(0.55 P_c, P_b) \quad (21)$$

$$\text{Homogeneous frozen flow ref. [2]:} \quad j = \frac{\sqrt{\frac{2}{\gamma+1} \frac{\dot{q}_s X_{sc} R_s T_c}{\left(\dot{q}_s v_{s1}^1 + \dot{q}_s (1 - X_{sc}) v_{s1}^1 + X_{sc} R_s \frac{T_c}{\rho} \right) \rho}}}{\text{with } \rho = \left(\frac{2}{\gamma+1} \right)^{\frac{\gamma}{\gamma-1}}} \quad (22)$$

10. Constraint Models

$$\text{Slug Expansion:} \quad \dot{V}_b = A_x (\dot{z} + u_e) \quad \text{with } \ddot{z} = \frac{P_b - P_c}{2l \cdot S_{Na}} \quad (23)$$

$$\text{Hemispherical Expansion:} \quad \dot{V}_b = 2\pi \tilde{r}_b^2 \cdot \dot{\tilde{r}}_b \quad \text{with } \ddot{\tilde{r}}_b = \frac{1}{\pi b} \left[\frac{P_b - P_c}{S_{Na}} - \frac{3}{2} \dot{\tilde{r}}_b^2 + u_e \left(\dot{\tilde{r}}_b + \frac{1}{2} u_e \right) \right] + \dot{u}_e \quad (24)$$

Volume increase by entrainment is accounted for in eq. (23) and (24) which required some generalization of the Rayleigh equation. Transition from one constraint model to the other either with constant kinetic energy of sodium or constant expansion rate of the bubble.

11. Bubble Pressure

$$P_b = P_{sat,s} \left(\frac{r_{sb}}{r_b} \right) + \frac{X_{Na} \dot{Q}_{Na} \rho_{Na} T_{sb}}{V_{gas}} \quad (25)$$

12. Covergas Pressure

$$P_t = P_{t0} \left(\frac{V_{t0}}{V_{t0} - V_{gas}} \right)^{1.667} \quad (26)$$

13. Sodium Entrainment

Cho ref [2_7] : $\dot{G}_{Na} = w \dot{G}_b$ non mechanistic with entrainmentparameter w as input (27)

Corradini
ref [3_7] : $\dot{G}_{Na} = S_{Na} U_e \begin{cases} AX & \text{for slug expansion} \\ 2\pi r_b^2 & \text{for hemispherical expansion} \end{cases}$ (28)

$$U_e = C \cdot [\max(ACC, 0)]^{1/4} \text{ with } C = 4.65 \sqrt{2\pi r_b^2 \frac{G}{S_{Na}}} \quad (29)$$

ACC is the acceleration at the vapor liquid interface of the bubble. For slug expansion

$$ACC = \frac{P_b - P_t}{Z \cdot S_{Na}} \quad (30)$$

For hemispherical expansion ACC is determined implicitly from the transcendent equation

$$F(ACC) = \frac{P_b - P_t}{S_{Na}} - \frac{3}{2} \tau_b^2 + C \tau_b ACC^{1/4} + \frac{1}{2} C^2 ACC^{1/2} - \tau_b ACC = 0 \quad (31)$$

14. Nomenclature

Indices

b = bubble region	L = latent heat of vaporization
c = pool or core region	p = pressure
e = entrainment	\dot{Q}_1 = heat rate for heating up and vaporizing subcooled sodium
f = f-component used only if steel is working fluid	\dot{Q}_m = heat rate for superheating of sodium vapor
Na = sodium	$\dot{Q}_{s,Na}$ = rate of heat exchange between s-component and entrained sodium
s = s-component (working fluid for blow-down)	q = power density per unit mass
t = covergas	R = special gas constant
o = initial value	R_D = average radius of entrained sodium droplets
' = saturated liquid	r_b = bubble radius
" = saturated vapor	T = Temperature

Symbols

ACC = Acceleration at the bubble liquid interface	u_e = entrainment velocity
AE = ejection orifice from the pool	v = volume
AX = Accelerated slug cross section	v = specific volume
C = Corradini constant	w = entrainment parameter
c = specific heat of liquid	x = vapor quality
C_G = specific heat of gas	ZI = inertial length of sodium slug
e = specific internal energy	z = coordinate for slug motion
G = mass	α_{gNa} = thermal diffusivity of sodium vapor
GREF = effective absolute gas constant in bubble	γ = isentropic exponent for vapor of s-component
H = constant in sodium vapor pressure equation	ϵ_r = radiative absorptivity of the sodium droplet surface
heff = effective heat exchange coefficient between f- and s component	ξ = mass fraction relative to G_b or G_c
j = blow down mass flux	ρ = density
K = constant in sodium vapor pressure equation	σ = surface tension of sodium
k_{gNa} = thermal conductivity of sodium vapor	σ_r = Stephan Boltzmann constant